




OPEN PLATFORM FOR REALIZING ZERO DEFECTS IN CYBER PHYSICAL MANUFACTURING


**D3.3 - Methodology for calibration and
uncertainty analysis and preliminary results**



Version	1.0
WP	3
Delivery Date	30/11/2023
Dissemination level	PU
Deliverable lead	UNIVPM
Authors	UNIVPM, USIT, TECNALIA, COMAU, AIMEN
Reviewers	AIMEN, LMS
Abstract	This document addresses the methodologies for calibration of the instrumentation embodied in the NDIs developed for the project. Calibration and uncertainty are fundamental topics for assuring the quality of measured data and the quality of diagnosis issued by NDIs. Therefore, Chapter 1 outlines the state-of-art on instrument calibration and uncertainty analysis in a general way, applicable to all NDIs. Chapters 2, 3 and 4 treat the specific aspects of calibration and uncertainty for the three measurement technologies that are being developed and implemented in the project. The way each technology can be calibrated is specified concerning the industrial applications developed for the various use cases. Lastly, the path for implementation of the NDIs in each use case and draws concluding remarks for each NDI under development is outlined.
Keywords	Calibration. Measurement uncertainty. Quality of measured data.
License	 <p>This work is licensed under a Creative Commons Attribution-NonCommercial 4.0 International License (CC BY-NC 4.0). See: https://creativecommons.org/licenses/by-nc/4.0/</p>

Dissemination Level:	
PU	Public, fully open
SEN	Sensitive, limited under the conditions of the Grant Agreement
Classified R-UE/EU-R	EU RESTRICTED under the Commission Decision No2015/444
Classified C-UE/EU-C	EU CONFIDENTIAL under the Commission Decision No2015/444
Classified S-UE/EU-S	EU SECRET under the Commission Decision No2015/444
Type	
R	Document, report (excluding the periodic and final reports)
DEM	Demonstrator, pilot, prototype, plan designs
DEC	Websites, patents filing, press & media actions, videos, etc.
DATA	Data sets, microdata, etc.
DMP	Data management plan
ETHICS	Deliverables related to ethics issues.
SECURITY	Deliverables related to security issues
OTHER	Software, technical diagram, algorithms, models, etc.




Co-funded by the European Union

Funded by the European Union. Views and opinions expressed are however those of the author(s) only and do not necessarily reflect those of the European Union or EUROPEAN HEALTH AND DIGITAL EXECUTIVE AGENCY (HADEA). Neither the European Union nor the granting authority can be held responsible for them.

Version History

Version	Date	Owner	Author(s)	Changes to previous version
0.1	2023/07/07	UNIVPM	UNIVPM	Outline
0.2	2023/09/19	UNIVPM	UNIVPM	First draft
0.3	2023/09/21	UNIVPM	UNIVPM	Contributions to partners required
0.8	2023/10/06	UNIVPM	UNIVPM, USIT, AIMEN, TECNALIA, COMAU	Contribution of most partners received
0.9	2023/11/07	UNIVPM	UNIVPM, USIT, AIMEN, TECNALIA, COMAU, AIMEN	All contributions received and harmonized, abstract and executive summary written
1.0	2023/11/30	UNIPVM	LMS	Full draft

Table of Contents

Version History	3
Table of Contents.....	4
List of Abbreviations & Acronyms	6
List of Figures.....	7
List of Tables	8
Executive Summary	9
1 Introduction to calibration and measurement uncertainty	10
1.1 Model of measurement systems	10
1.2 Measurement uncertainty.....	10
1.3 The evaluation of uncertainty according to GUM	14
1.3.1 Type A evaluation of uncertainty	14
1.3.2 Type B evaluation of uncertainty.....	15
1.4 Uncertainty and conformity assessment.....	16
1.5 Calibration procedure.....	17
2 Uncertainty and calibration methodology for laser line triangulation instruments for geometry measurement 19	
2.1 Uncertainty of laser line triangulation systems.....	19
2.2 Methods for calibration of laser line triangulation systems	20
2.2.1 Calibration method for laser line triangulation NDI systems for bar straightness.....	21
2.2.2 Calibration method for laser line triangulation NDI system for gap and flush measurement	22
2.2.3 Calibration method for 3D geometry measurement NDI system with laser line triangulation	23
3 Uncertainty and calibration methodology for vision-based techniques (VIS and IR) for in-line defect detection 23	
3.1 Uncertainty in vision systems	24
3.2 General methods for vision systems calibration	26
3.2.1 Spatial calibration of vision systems.....	26
3.2.2 Intensity calibration of infra-red vision systems	27
3.2.3 Intensity calibration for NDIs exploiting neural networks.....	28
4 Uncertainty and calibration methodology for X-ray instrumentation for residual stress developed.....	28
4.1 Uncertainty of X-ray Residual Stress measurement.....	31
4.1.1 Uncertainty related to statistical processing.....	31
4.1.2 Effect of system misalignment on stress results:	31
4.1.3 Effect of specimen displacement:.....	32
4.2 Calibration of X-ray residual stress measurement	32
5 Pathway for implementation and concluding remarks	33
References	34

List of Abbreviations & Acronyms

CMM	:	Coordinate Measuring Machine
FN	:	False Negative
FOV	:	Field of View
FP	:	False Positive
GUM	:	Guideline for the estimation of uncertainty in Measurement
KPI	:	Key Performance Indicator
LLT	:	Laser Line Triangulation
NDI	:	Non-Destructive Inspection system
VIM	:	International Vocabulary of Metrology
WP	:	Work Package

List of Figures

Figure 1: Block representation of a measurement system	10
Figure 2: Ideal model of a measurement system	10
Figure 3: Disturbances acting on the measurement system	11
Figure 4: Conceptual description of uncertainty affecting a measurement	12
Figure 5: From measurement uncertainty to quality of decisions	13
Figure 6: Quality control in production lines	13
Figure 7: Gaussian distribution of repeated measurements of x_i	14
Figure 8: Standard uncertainty and expand uncertainty	15
Figure 9: Result of a measurement, expressed as an interval of values.	16
Figure 10: Uncertainty and conformity	16
Figure 11: Specification vs. conformity range	16
Figure 12: a) Plot of calibration data and linear fit of a straight line,.....	18
Figure 13: a) Laser Line Triangulation sensor (image from Stemmer Imaging).....	19
Figure 14: Schema of an LLT sensor: a) the LLT sensor, b) the acquired image, c) the conceptual model.	20
Figure 15: Determination of the centroid of the laser line at a generic column j	20
Figure 16: Typical calibration plots for LLT sensors [8]	21
Figure 17: Examples of calibration targets used for LLT sensors (References: figure (a) [9], figure (b) [10], figure (c) [11], figures (d), (e), (f) [12]	21
Figure 18: Schematic of zigzag face calibration [13]	22
Figure 19: Laser line triangulation NDI systems for bar straightness Calibration bench (prototype version) (a); detail of the calibration target (b)	22
Figure 20: NDI#8 target geometry	23
Figure 21: NDI#8 calibration bench.	23
Figure 22: NDI for 3D geometry measurement architectur	23
Figure 23: Example of typical image distortions.....	25
Figure 24: Problems related to absorption, transmission, and reflection	25
Figure 25: Uncertainty due to radiation absorbed in the path from the object to the sensor	26
Figure 26: a) Example of interfering radiation sources: reflected (orange path) and transmitted radiation (blue path). b) Solutions against environmental interference	26
Figure 27: a) Checkerboard for visible systems, b) checkerboard for infrared systems, c) infrared image of the checkerboard for infrared systems.....	27
Figure 28: Role of extrinsic and intrinsic parameters image formation	27
Figure 29: a) UNIVPM emissivity calibration setup. b) Partially painted sample. c) Setup for heating the sample.	28
Figure 30: Direction of measurement in x-ray diffraction where n : = reflection order, λ : = wavelength, d : = distance between two planes oriented according to (hkl) and θ : = angle of diffraction [17].....	29
Figure 31: iXRD system with modular mapping	29
Figure 32: Distribution forces, and the stresses they cause, on the forces of a homogeneously loaded unit cube at static equilibrium. Schematic representation of tensional state at one point (a) and principal stress and directions at the same point 18.....	30
Figure 33: " 2θ vs. $\sin^2\Psi$ curve, calculation of normal stress" and shear stress.....	31
Figure 34: Effect of beam shift and sample translation on the shape of $\sin^2\Psi$ curve, and Ψ -mode.	31
Figure 35: Effect of beam shift and sample translation on the shape of $\sin^2\Psi$ curve, and Ω -mode.....	31
Figure 36: Good alignment [20].....	32
Figure 37: The system is out of alignment and needs to be moved up [20]	32
Figure 38: The system is out of alignment and needs to be moved down and left [20].....	32

List of Tables

Table 1: Example of calibration coordinates (q_i, q_0)	18
--	----

Executive Summary

The purpose of this document is to underline the importance of instrument calibration and uncertainty analysis for the acquisition of reliable data and the delivery of accurate diagnosis. Indeed, we measure to make decisions based on data, therefore the quality of data is of fundamental relevance for any decision-making process based on measured data. And quality of data fully relies on the quality of measurement instrumentation and on its appropriate use; in industrial environments, where disturbances are always present, the question of assessing measurement uncertainty is therefore very relevant.

This is why Deliverable 3.3 addresses the methodologies for calibration of the instrumentation embodied in the NDIs developed for the openZDM project. Calibration and uncertainty are the fundamental aspects to be carefully considered for assuring the quality of measured data and the quality of diagnosis issued by NDIs based on experimental measurements.

In the context of Zero-Defect Manufacturing, and more in general when dealing with management strategies based on data, measurement science is seldom mentioned as a key technology. However, we aim to underline that it has to be considered to all extents as an enabling technology for any management strategy that employs measured data. Instead, too often, measurement science is considered either a topic for metrologists and metrology institutions or considered a mature and fully reliable technology, that one can plug and play with no difficulty.

Hence, the focus of this deliverable is put on instrument calibration and measurement uncertainty, and about the NDIs under development and being applied to the use cases of the openZDM project.

In order to harmonize the way these concepts are treated in the next chapters and to establish a common language, Chapter 1 outlines the state-of-the-art instrument calibration and uncertainty analysis in a general way, applicable to any type of measurement instrument and all NDIs.

The following Chapters 2, 3 and 4 then treat the specific aspects of calibration and uncertainty for the three measurement technologies that are being developed and implemented in the project, namely Laser Line Triangulation, vision in visible and infrared spectra, and x-ray testing. The way each technology will be calibrated is specified, taking into account the industrial context, the scope of the measurement, and the constraints that the industrial applications of the various use cases pose.

This document finally outlines the path for implementation and draws some concluding remarks addressing each NDI under development.

1 Introduction to calibration and measurement uncertainty

1.1 Model of measurement systems

A measurement system is a device whose function is to measure an input quantity q_i and provide an output q_o , related to that input. The input quantity q_i is named the “measurand”: it is indeed the physical quantity that you are interested in. The output quantity q_o of an analogue sensor is in most cases an electric analogue signal, a voltage or a current; however, there exist digital sensors, whose output is a numeric value. Figure 1 is a schematic representation of the measurement system.



Figure 1: Block representation of a measurement system

The “observer” receives the output quantity q_o , but is interested to know the value of the input quantity q_i ; this is possible if the relationship between output quantity q_o and input quantity q_i is known. This relationship can be represented as expressed in Eq. 1:

$$q_o = f(q_i) \tag{Eq. 1}$$

Eq. 1 is a model of the ideal behaviour of the sensor and is represented in Figure 2. This model can be determined experimentally through the calibration of the sensor; calibration therefore emerges as the fundamental procedure which allows to use of an instrument to perform a measurement of an unknown input quantity. The relationship $q_o = f(q_i)$ is the calibration function.

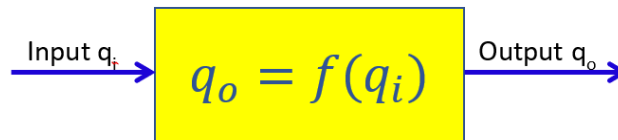


Figure 2: Ideal model of a measurement system

When measuring by using a sensor, the “observer” will detect the output quantity q_o and, by inverting Eq. 1, he will determine the input quantity q_i he is interested in; Eq. 2 describes this process.

$$q_i = f^{-1}(q_o) \tag{Eq. 2}$$

Once the result of a measurement is obtained, it has to be written as the numerical value of that quantity q_i , expressed in a unit of the SI (International System of Units).

1.2 Measurement uncertainty

However, the model of a measurement system outlined above in Eq. 1 and Eq. 2 is an ideal description of the behaviour of a measurement system. Indeed, many factors influence the measurement process so that measurements are always affected by uncertainty.

Causes of uncertainty are many and are related mainly to:

- a) the way we model the measurement process;
- b) the effect of disturbances over the measurement process.

In fact, whenever we take some measurements, the first step is to model the measurement. This model is always an imperfect representation of the reality. This implies that the quantity we want to measure, the input quantity

q_i , is ill-defined. Two examples can describe how modelling the measurand in real applications introduces uncertainty in the measurement process:

- **Example 1:** Measurement of the length of a steel bar. When doing this geometrical measurement, we immediately associate a geometrical model with the bar. In the case of a straight bar, the model that we will generally adopt is a square angle parallelepiped. Of this geometrical figure, we will measure length, height and width. But are we sure that the bar shape matches exactly the shape of a parallelepiped? Any deviation from that shape will determine uncertain measurements of length, height and width.
- **Example 2:** Measurement of the temperature of a body. Again, when doing such measurement, we could assume that the object has a uniform temperature, which we call the temperature of the body. We measure temperature at one point, and attribute it to the whole body. But are we sure that body temperature is uniform? Any deviation from this assumption will cause uncertainty in the measurement of temperature.

Model-related uncertainty relates also to uncertain modelling of the measurement system. Eq. 1 is indeed an uncertain representation of the measurement system.

In addition to model-related uncertainty, any measurement system suffers from the effects of disturbances. Disturbing inputs act on the instrument and affect negatively its performance. Two main categories of disturbing inputs are generally identified:

- Interfering inputs – their effect is to produce variations of the output quantity q_o which are not caused by the input quantity q_i ; therefore, the output quantity q_o may change even if the input quantity q_i does not change. In practice they act in an additive way on the output, adding or subtracting content to the output signal. A typical example is electromagnetic noise affecting a sensor; electromagnetic disturbances may induce spurious voltage which adds up to the output quantity q_o , thus causing uncertain measurements.
- Modifying inputs – their effect is to modify the functional relationship $q_o = f(q_i)$. If the function f changes, the computation of the input quantity q_i through inversion of the calibration function produces errors. A typical example of modifying input is temperature variations acting over an elastic force transducer; if temperature changes, the stiffness of the elastic transducer changes, thus modifying the input-output relationship and causing uncertain measurements.

Both interfering inputs and modifying inputs can be random or systematic. In the case of random disturbances, the output of the measurement system will fluctuate randomly, while in the case of systematic disturbances, the output will be affected by bias, i.e. a systematic shift of the measurement. Bias, if known, can be corrected.

These concepts can be depicted in Figure 3; it shows that the output signal is not only determined by the input quantity q_i , but also is affected by uncertainty.

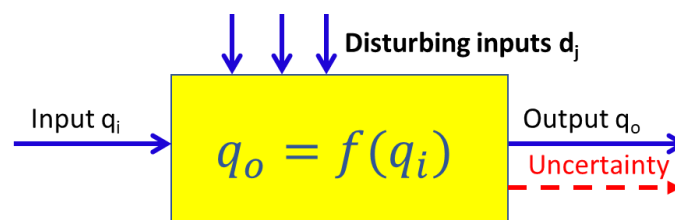


Figure 3: Disturbances acting on the measurement system

The following Eq. 3 can be used to describe what happens in a real measurement taken by a real instrument.

$$q_o = f(q_i, d_1, d_2, \dots, d_j, \dots) = f'(q_i) \pm \text{UNCERTAINTY} \quad \text{Eq. 3}$$

Figure 4 summarizes these concepts and synthetically represents them. Note that disturbances act independently from our control, may be random or systematic, and several disturbances d_j may act simultaneously; the modifying disturbances modify the calibration function f into f' , while the interfering disturbances add up undesired contributions to the output quantity. Overall, this affects the measurement and produces uncertainty in measurement, which may be a combination of random and systematic effects.

If one would know the systematic effects, i.e. if one would know f' , systematic effects could be compensated for. Instead, random effects by nature act in a chaotic way, and therefore, cannot be compensated and can be

estimated only through statistics. Averaging multiple measurements reduces the effect of random disturbances because they generally have zero mean.

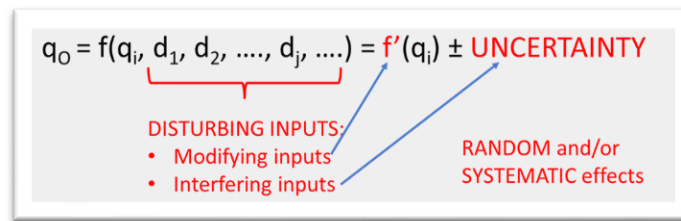


Figure 4: Conceptual description of uncertainty affecting a measurement

Disturbances are therefore a problem to be addressed when designing an instrument and whenever taking measurements. In a very concise manner, we can say that:

- the designer/manufacturer of an instrument should minimize its sensitivity to disturbances; an ideal instrument is in fact sensitive only to the input quantity q_i that you desire to measure. In any real instrument, minimizing sensitivity to disturbances will reduce their effect, and hence will reduce uncertainty in measurement. Each type of sensor technology requires specific solutions to achieve this goal.
- disturbances should be filtered in input, if feasible so that they do not reach the instrument – for example, if a load cell measuring weight suffers from the effect of vibrations, vibrations should be filtered by appropriate spring-damper supports, which act as a mechanical filter.
- in some cases, the effects of disturbances on the output can be filtered out, so to remove their contribution – for example, this is the case of electromagnetic disturbances caused by the electric power network, which in Europe operates at 50 Hz; an output signal q_o containing oscillations at 50 Hz or its harmonics, highly probably is affected by electromagnetic disturbances, removable by notch filters operating at 50 Hz and harmonics. Of course, filtering the output signal is possible only if we are confident that the desired information does not lie in the same frequency band.

Evaluating uncertainty, and compensating for systematic effects, when possible, is therefore fundamental for taking good quality measurements. Calibration is the procedure through which we determine the model of the measurement system and the associated uncertainty. Therefore, instrument calibration and evaluation of measurement uncertainty are two fundamental steps to be performed when taking data through measurements.

A vast literature exists on uncertainty evaluation; in this Deliverable, we refer to the guidelines released by metrology institutes and standardization bodies, in order to adopt a commonly agreed way to treat this complex topic. It is important to note here that, even if standardized approaches to the evaluation of uncertainty in measurement have existed for more than a decade and are available through standardization bodies, their actual use in industry is still lagging; data about uncertainty are not always provided in agreement with the guidelines, therefore treating data about uncertainty in industrial applications (but not only) is still an “uncertain process”!

The Joint Committee for Guides in Metrology (JCGM) [1], chaired by the Director of the Bureau Internationale de Poids et Mesures (BIPM) [2], was formed in 1997 and produced a synthesis of the many activities carried out by national metrology institutes and the ISO Technical Advisory Group 4 (TAG 4) which led to the publication a series of guides about uncertainty estimation, the so-called GUM series [3]. In this series, the main documents are the *Guide to the Expression of Uncertainty in Measurement (GUM)* [4] and the *International Vocabulary of basic and general terms in Metrology (VIM)* [5].

In the introduction to the GUM series, JCGM writes:

“uncertainty is a measure of the quality of a measurement and can be vital in many cases. The JCGM/100 series of documents establishes general rules for evaluating and expressing uncertainty in measurement that can be followed at various levels of accuracy and in many fields — from the shop floor to fundamental research. Therefore, the principles of these Guides are intended to be applicable to a broad spectrum of measurements, including those required for:

- *maintaining **quality control** and quality assurance in production.*
- *complying with and enforcing laws and regulations.*
- *conducting basic research, and applied research and development, in science and engineering.*

- *calibrating standards and instruments and performing tests throughout a national measurement system to achieve traceability to national standards.”*

In that text, two concepts have been highlighted, which are very relevant for the openZDM Project: evaluating measurement uncertainty is fundamental to maintaining quality control in production, and calibration of the instruments is necessary for this scope, thus, why uncertainty and calibration are important for in-line quality control.

A few logical steps bring to the evidence that whenever dealing with data, measurement uncertainty needs to be estimated and instruments need to be calibrated:

1. **one measures to make decisions** based on experimental evidence.
2. **quantitative data** about physical quantities originate through **measurement processes**.
3. **measuring instruments**, due to their nature, to their complex interaction with the measurand and the measurement environment, **produce data** that are always intrinsically affected by **uncertainty**.
4. hence, **uncertainty of measurement** affects the **level of confidence in decisions** made based on uncertain data.
5. it is therefore essential to guarantee the **quality of the data**; this implies the ability to **understand** and **manage** the entire **measurement process**, to use **calibrated instruments**, and to pay attention to **disturbances** affecting the measurement process.

The ISO standard ISO-10012:2003: “Measurement management systems – Requirements for measurement processes and measuring equipment” [6] provides an answer to the question “Why should one calibrate a measurement system?”. It explains that calibration is part of “..... *the set of operations required to ensure that measuring equipment conforms to the requirements for its intended use ...*”

Overall, dealing with measurement uncertainty and calibration means dealing with the quality of the measured data and the level of confidence in all decisions that will be taken based on those data (Figure 5).

The whole paradigm of Zero-Defect Manufacturing (ZDM), and more in general of Industry 4.0, rely on data; good quality data are available only if we perform good quality measurements. This is why measurement science, in this context, is to be considered an enabling technology.

Measured data should always be expressed and used taking into account their uncertainty.

The role of measurement systems for quality control in production lines takes place in the so-called quality control stations (Figure 6); the quality control station contains at least one measurement system that takes measurements and provides data to be used for conformity assessment. A properly calibrated instrument and a sound evaluation of uncertainty allow us to optimize the quality control process and enforce all following decisions. A properly operating quality control station impacts positively both process efficacy and production efficiency, as well as customer satisfaction, overall reducing costs on non-quality.



Figure 5: From measurement uncertainty to quality of decisions

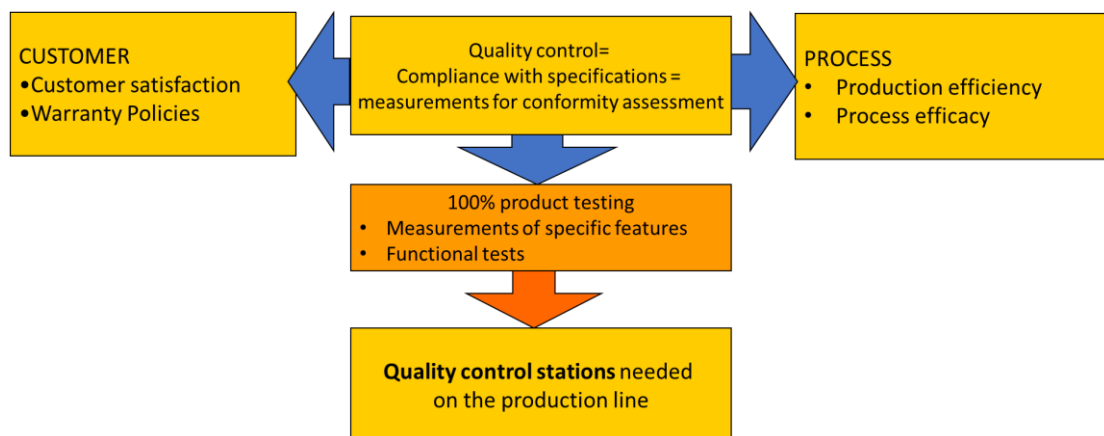


Figure 6: Quality control in production lines

1.3 The evaluation of uncertainty according to GUM

The GUM describes various methods for the evaluation of uncertainty, which can be grouped into two types:

- Type A – evaluation of uncertainty based on statistical analysis of repeated measurements;
- Type B – any other method which is not Type A.

1.3.1 Type A evaluation of uncertainty

Assuming one repeats N times the measurement of the input quantity $q_i = x_i$, a statistical analysis of the distribution of x_i allows an estimate of uncertainty. Of course, the input quantity should be stationary, i.e. should not change over time.

In particular, being the measurements of x_i affected by uncertainty, each repetition will provide a slightly different value. If the causes of uncertainty are many and are acting independently from each other, the distribution of measures will be random and it will tend to a Gaussian shape as represented in Figure 7 (this applies in case of an infinite number of measures N , of course in real applications N is always finite and often small, down to $N=1$).

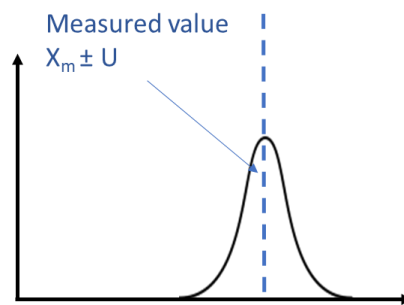


Figure 7: Gaussian distribution of repeated measurements of x_i

GUM proposes to compute the arithmetic mean \bar{x}_m and use it as the final result of the measurement (Eq. 4).

$$\bar{x}_m = \frac{\sum_{i=1}^N x_i}{N} \quad \text{Eq. 4}$$

The arithmetic mean \bar{x}_m is the best estimate of the measurand, the input quantity. It is important to note that this is feasible only for stationary (or periodic) quantities and in any case, it is a time-consuming procedure. Indeed, in many applications, only one measurement is taken ($N=1$), so that the arithmetic mean coincides with the only measure available.

Then GUM proposes to evaluate uncertainty considering the amplitude of the distribution of the repeated measurements. For this purpose, GUM proposes to compute the standard deviation s_x and use it as the estimate of the standard uncertainty $u(x)$, through the following formula reported in Eq. 5:

$$u(x) = s_x = \sqrt{\frac{\sum_{i=1}^N (x_i - \bar{x})^2}{N - 1}} \quad \text{Eq. 5}$$

If the final result of the measurement is the arithmetic mean \bar{x}_m , then its standard uncertainty $u(\bar{x})$ can be computed according to Eq. 6:

$$u(\bar{x}_m) = \frac{s_x}{\sqrt{N}} \quad \text{Eq. 6}$$

However, if uncertainty would be expressed using standard deviations, in a Gaussian distribution only about 68% of data would fall within a range of $\pm u(\bar{x})$ centered around \bar{x}_m . This would limit the confidence level on the result of the measurement. For this reason, GUM suggests to use the expanded uncertainty (Eq. 7):

$$U(\bar{x}_m) = k u(\bar{x}_m) \quad \text{Eq. 7}$$

where the factor k , named coverage factor should be $k=2$, thus allowing for 95% of data to fall within an interval $[\bar{x}_m \pm U(\bar{x}_m)]$, as visible in Figure 8; this expression represents the final result, including the expanded uncertainty $U(\bar{x}_m)$.

Of course, all figures should be expressed in proper SI units and the SI unit should be indicated explicitly.

It is important to note that if $N=1$, the standard uncertainty cannot be computed by a series of measurements and the result of the measurement will be the only datum available, x ; one should use the information available through previous tests, allowing to estimate the standard deviation of the population $u(x)$ and the expanded uncertainty $U(x)$, and express the result as $[x \pm U(x)]$.

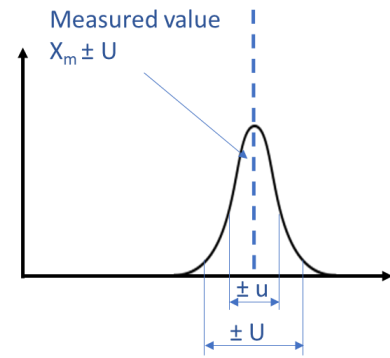


Figure 8: Standard uncertainty and expand uncertainty

1.3.2 Type B evaluation of uncertainty

Type B uncertainty estimates are based on other methods, not on repeated measurements of a constant input.

One common approach, particularly useful in the phase of instrument design when the instrument does not exist physically, is to use a model of the measurement system. The model should describe the relationship between input x_i and output x_o and take into account design parameters p_j ($j=1, \dots, M$) and the other variables acting on the instrument, possibly all disturbing inputs d_k ($k = 1, \dots, K$). A model could be written as (Eq. 8):

$$x_i = g(x_o, p_1, \dots, p_M, d_1, \dots, d_K) = g(z_1, \dots, z_N) \quad \text{Eq. 8}$$

where z_l ($l=1, \dots, N$) represents a generic variable, either a parameter or a disturbance, which has an influence on the instrument behaviour.

The variance $s_{x_i}^2$ of the measured quantity x_i can then be computed if it is known (or hypothesized) the variance of each variable z_l appearing at the right of equation (Eq. 8); under the assumption of small variations and independence of all terms, the following expression combines all variances s_{z_l} and allows to estimate the standard deviation s_{x_i} (Eq. 9).

$$s_{x_i} = \sqrt{\sum_{l=1}^N \left(\frac{\partial g}{\partial z_l} s_{z_l} \right)^2} \quad \text{Eq. 9}$$

Once s_{x_i} is known again the expanded uncertainty is computed as $U(x_i) = 2u(x_i) = 2s_{x_i}$.

The model (Eq. 8) can also be used in a Montecarlo simulation; multiple estimates of x_i can be sequentially computed by simulating fluctuations of the variables z_l of the model, either parameters or disturbances. This would produce an artificial statistical distribution, over which statistics allows us to evaluate uncertainty by computing arithmetic mean and standard deviation.

The guideline GUM allows also to implementation of other methods for Type B estimates of uncertainty, based on previous knowledge or on calibration certificates etc.; the options are several, but we have discussed only the main ones commonly adopted in industrial applications.

Finally, it is worth saying that GUM indicates to compute combined standard uncertainty; combined standard uncertainty is the uncertainty resulting from the superposition of different uncertainties. It is computed as the square root of the sum of squared standard uncertainty components. This algorithm is also known as 'Summation in Quadrature' or 'Root Sum of the Squares'. For example, in a force transducer one should combine calibration uncertainty with uncertainty due to temperature variations, if in the application the transducer will undergo temperature variations which were not accounted for during the calibration, typically done in controlled temperature environments.

1.4 Uncertainty and conformity assessment

As previously mentioned, the result of a measurement should be expressed as an interval of possible values that the measurand probably has (Figure 9).

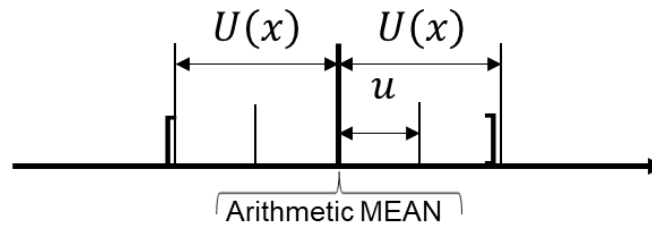


Figure 9: Result of a measurement, expressed as an interval of values.

This fact has a relevant role in conformity assessment, i.e., in the process of verifying if the measured value falls within specifications or not. Conformity assessment is the step in which the result of the measurement is compared to specifications; the output should be a diagnosis, i.e., conformity (OK) or non-conformity (KO). However, being the measurements uncertain, the diagnosis can be uncertain too.

The following Figure 10 shows two possible situations. On the left, it is represented the distribution of repeated measurements of an instrument with expanded uncertainty U_L , while on the right it is represented the distribution of measurements of an instrument with expanded uncertainty U_S . The uncertainty U_L is large, while U_S is small.

If we take only one measurement, we may obtain the value x_1 ; let's compare what would happen if both instruments measure x_1 ; the value x_1 has been on purpose represented close to the upper specification limit, the red line on the right of each plot. Having a large uncertainty U_L , for the instrument on the left we need to assume a large uncertainty interval; part of it falls outside the specification range. Assuming a Gaussian distribution, the probability of falling outside specifications is represented by the dark area, which is not negligible. It means that even if x_1 is within the specifications, the probability that instead the actual value of x falls outside is not negligible. If the diagnostic question is "is the measured sample a defect?" being x_1 within the specifications the answer would be "negative"; however, there is a non-negligible probability that instead the sample is "positive". If this were true, we are in front of a case of "false negative", i.e., the diagnosis would not be correct.

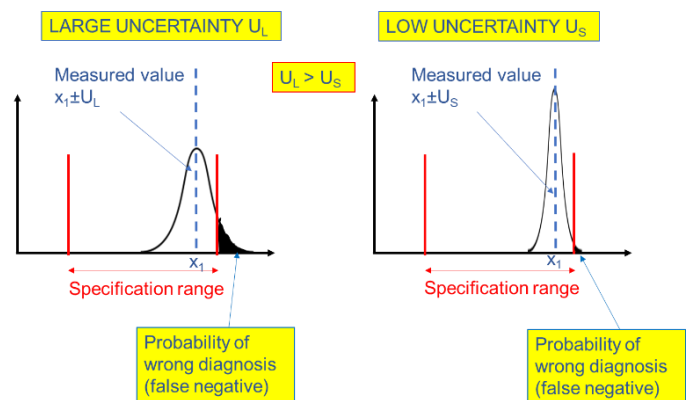


Figure 10: Uncertainty and conformity

On the right of Figure 10 instead, we see that the instrument has a much smaller uncertainty U_S . The plot shows that the probability of a "false negative" is much smaller (the black area under the curve at the right).

Of course, diagnostic errors may occur, either "false negatives – FN" or "false positives – FP". FP would happen when the measurement x_1 lays outside the "specification range", but the Gaussian distribution has tails that fall within it; again, if expanded uncertainty U is small this is less likely to occur.

What has been commented through this example, can be generalized. If measurement uncertainty increases, then conformity assessment will be more uncertain. Figure 11 shows the situation, as it is described in the ISO standard about conformity assessment of geometric measurements [7] (the same approach can be applied to any type of measurement): if one wants to assess conformity by minimizing risks of false diagnosis to lower than 5%, conformity should be

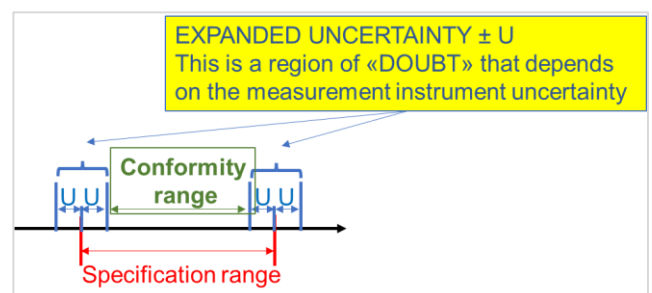


Figure 11: Specification vs. conformity range

assessed only within the “conformity range”, which is smaller than the specification range and it is computed as the “specification range (T)” minus two times the expanded uncertainty U. Of course, if uncertainty U is large, the “conformity range” will become small; this is why empirical considerations suggest that U should be an order of magnitude smaller than the “specification range (T)” and in any case it is highly suggested that the ratio U/T should not exceed 1/4.

This discussion has been carried out for bilateral specifications, a tolerance interval imposed to a quantity under control. Of course, similar reasoning applies in the case of uni-lateral specifications, either an upper threshold or a lower threshold.

1.5 Calibration procedure

The International Vocabulary of Metrology (VIM) [5] defines calibration as: “operation that, under specified conditions, in a first step, establishes a relation between the quantity values with measurement uncertainties provided by measurement standards and corresponding indications with associated measurement uncertainties and, in a second step, uses this information to establish a relation for obtaining a measurement result from an indication.

A calibration may be expressed by a statement, calibration function, calibration diagram, calibration curve, or calibration table. In some cases, it may consist of an additive or multiplicative correction of the indication with associated measurement uncertainty.”

It is not an easy and operative definition!

To better understand its meaning it is important to highlight some words:

- “operation that”: this means that calibration is a procedure;
- “under specified conditions”: this means that the result will apply if the specific conditions are met;
- “establishes a relation between”: this means that the result of a calibration procedure will be a relation;
- “between ... quantity values ... provided by measurement standards ... and corresponding indications”: this means that the result will be a function between the values of the output quantity of the instrument q_o and known values of the input quantity q_i ;
- “measurement standards”: this implies that known values for the input quantity q_i must be available;
- “with associated uncertainties”: this means that calibration and uncertainty are strictly related to each other.

Then, in note 1 it is mentioned explicitly the “calibration function”, which can be used to express the result of a calibration procedure.

Hereafter the main steps to consider when calibrating an instrument are explained. The model of the instrument is $q_o = f(q_i)$ and it has been represented in Figure 2; this is the calibration function to be determined. The purpose of the calibration procedure is to determine the calibration function f and the associated uncertainty. The procedure will follow the steps:

- Examine the input range of the sensor to be calibrated and provide a series of N known values of the input quantity q_i , which lie within the input range and are possibly equally spaced so as to uniformly cover the input range. Reference values should be known with an uncertainty significantly lower than that of the instrument under calibration; an order of magnitude would be preferable. This can be done in different ways:
 - standard reference samples can be available for q_i – for example calibrated reference gauge blocks for dimensional measurements;
 - different values of q_i can be realized by specific equipment, the calibration bench, and measured with a reference instrument whose uncertainty is known and significantly lower than that expected for the instrument under test (an order of magnitude would be desirable).
- Measure one by one the known input values q_{ij} , and record the corresponding output of the sensor q_{oj} . Measurements should be taken in sequence, from the smallest to the largest and back; doing this, possible hysteresis will manifest itself. If we have N known input values, for each of them the measurement will be repeated twice; overall $2N$ points (q_{ij}, q_{oj}) will be available with $j=1, \dots, 2N$.
- Plot the points in a cartesian graph, with input quantity as abscissa and output quantity as ordinate.

- iv. Perform a least square linear regression of the data – for most instruments this is done by a straight line because instruments are usually designed to be linear; however, any order polynomial may be fit for the purpose, in case of non-linearities. The fitting function $q_o = f(q_i)$ represents the calibration function. Once this is known, the instrument can be used to determine q_i from the reading of q_o .
- v. Residuals of the calibration points with respect to the least square fit have to be computed and plotted; their scatter is due to measurement uncertainty during calibration, the so-called calibration uncertainty.
- vi. If the linear regression has been performed with a curve $q_o = f(q_i)$ having a proper shape, the residuals will be randomly scattered, with a zero mean value. If the residual plot shows trends, it means that the linear regression has to be improved and the model still does not represent the behaviour of the instrument. A general solution to this is to use a higher-order curve for the fitting of calibration data.
- vii. Considering residuals as random, their distribution should be Gaussian; therefore, one can compute the standard deviation of residuals and s_{q_o} and then estimate the expanded uncertainty of the output as $U_{q_o} = 2s_{q_o}$. From U_{q_o} we can then compute the expanded uncertainty for the:
- viii. input $U_{q_i} = \frac{U_{q_o}}{m}$; this is the calibration uncertainty of the instrument.

It is important to observe that calibration compensates for any systematic effect, therefore a calibrated instrument should not exhibit bias.

Table 1 reports a real example: the calibration of a pressure transducer, operating over an input range of q_i [0 ÷ 70] bar. The sensor output q_o is in volt [V]. The calibration function is expected to be linear, due to the working principle and the sensor design. Calibration has been done by providing known values of input pressure $q_{i,j} = (0, 10, 20, 30, 40, 50, 60, 70)[bar]$; these known reference values of input pressure have been generated by a deadweight tester, the classical calibration bench for pressure transducers. The table contains three columns, the index j of each calibration point and its coordinates (q_{ij}, q_{oj}) . The following Figure 12 reports the calibration data on a cartesian graph and the linear fit of a straight line $q_o = f(q_i) = mq_i + b$, whose equation is reported as well; m is the sensitivity of the sensor expressed in [V/bar]. It is evident that calibration data are close to the line, scattered around it. The plot of residuals is in Figure 12; it shows data randomly scattered around a zero mean; this is a qualitative indicator of a good linear fit. A classical test for normality could then be performed to have a quantitative verification of the findings.

Table 1: Example of calibration coordinates (q_i, q_o)

n°	qi [bar]	qo [V]
1	0	0
2	10	0,98
3	20	1,99
4	30	2,98
5	40	3,99
6	50	4,92
7	60	6
8	70	6,99
9	70	7,03
10	60	6,03
11	50	5,06
12	40	4,09
13	30	3,02
14	20	2,1
15	10	1,05
16	0	0,08

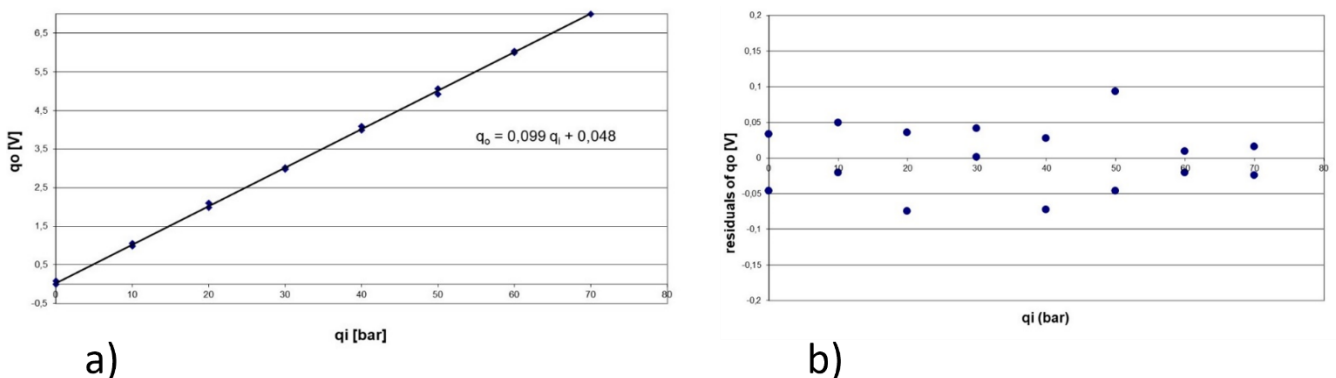


Figure 12: a) Plot of calibration data and linear fit of a straight line, b) Plot of residuals of the linear fit

The analysis of residuals allows us to compute an expanded uncertainty $U_{q_o} \cong \pm 0.09 V$, which in turn becomes $U_{q_i} = \frac{U_{q_o}}{m} \cong \pm 0.94 bar$.

In conclusion, the calibration procedure described above provides the model of the instrument and its calibration uncertainty.

In addition, calibration guarantees the metrological traceability of the measurement. Metrological traceability is defined by VIM as “..... *property of a measurement result whereby the result can be related to a reference through a documented unbroken chain of calibrations*”, which is a prerequisite for expressing measurement results as referred to the standard unit of measurement of the International System of Units, internationally known by the abbreviation SI (for *Système International*).

Calibrations can be done both by manufacturers and by calibration laboratories. In particular, when calibration is done by an accredited calibration laboratory, which operates according to the ISO/IEC 17025 standard [15], it will have a legal value.

2 Uncertainty and calibration methodology for laser line triangulation instruments for geometry measurement

In the context of openZDM, various NDIs are developed and applied making use of a specific class of optoelectronic sensors, namely Laser Line Triangulation systems (LLT). In the project four NDIs are under development embodying LLT sensors, designed for different applications and having different sizes and measurement ranges:

- A Laser line triangulation NDI system for bar straightness (bar at low temperature);
- Laser line triangulation NDI system for bar straightness (bar at high temperature);
- A 3D geometry measurement NDI system with laser line triangulation on a robot;
- An IIoT portable laser line triangulation NDI system for gap and flush measurement.

Any LLT has similar problems in taking measurements, sources of uncertainty are similar and calibration procedures are similar as well. Therefore, they are dealt with hereafter without focussing on a specific instrument.

2.1 Uncertainty of laser line triangulation systems

The general scheme of an LLT sensor is reported in Figure 13. It measures the profile $z(x)$ over a section of the object under test; the section is defined by the laser line projected onto it.

Each column of an LLT can be considered a single-point laser triangulation sensor. The measurement principle is triangulation; Figure 13 reports a geometrical model for a single-point laser triangulation sensor. LLT systems can be considered an array of single-point sensors, parallel to each other so that this 1D model applies also to them. In the single point model, the input quantity is the distance $q_i = \Delta z$, while the output quantity is the displacement of the image of the laser spot formed on the sensor $q_o = \Delta v$.

Triangulation sensors are slightly non-linear: Eq. 10 is the geometrical model of the instrument. The output quantity $q_o = \Delta v$ is measured in pixels, being the sensor discrete.

$$\Delta v = \frac{f X_o}{X_o - f} \left(\frac{\Delta z}{\frac{X_o}{\sin \alpha} - \frac{\Delta z}{\tan \alpha}} \right) \quad \text{Eq. 10}$$

Non-linearities are evident, therefore calibration will exploit a polynomial function.

Figure 14 shows the LLT sensor (a), the image of the laser line (b) and the conceptual block diagram (c). It is important to note that an LLT is a 2D sensor, whose input is a profile, i.e. a set of geometrical coordinates (x, z) and whose output is a set of pixel coordinates (i, j) , on which the laser line image forms. The correct detection of the pixel coordinates of the laser line image is therefore fundamental for the measurement and its uncertainty. Specific algorithms interrogate the acquired image column by column j and determine the centroid of the laser line (i, j) , as represented in Figure 15. Of course, this process requires a sufficiently contrasted image, which is not always the case, especially on surfaces which do not diffuse enough light. A significant part of the uncertainty in LLT sensors derives from insufficient or improper light scattering from the target surfaces.

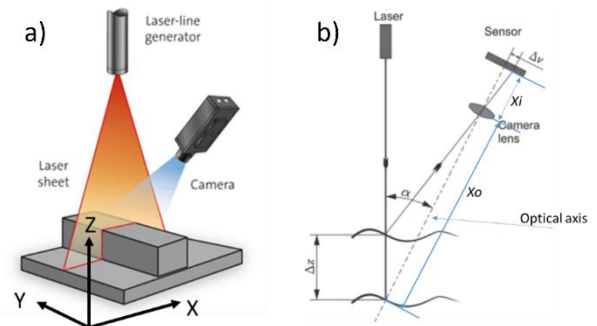


Figure 13: a) Laser Line Triangulation sensor (image from Stemmer Imaging)

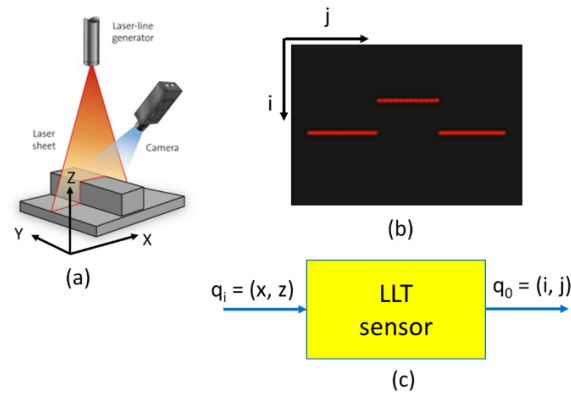


Figure 14: Schema of an LLT sensor: a) the LLT sensor, b) the acquired image, c) the conceptual model.

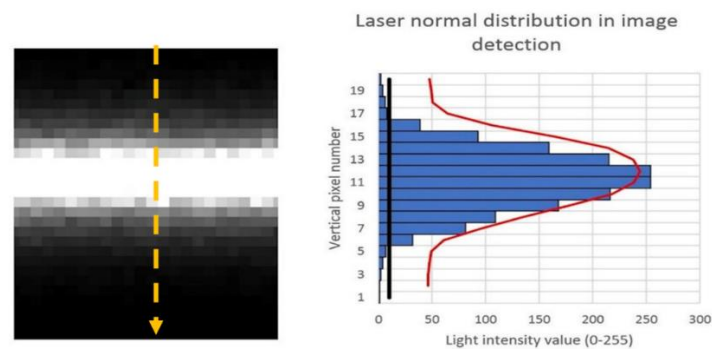


Figure 15: Determination of the centroid of the laser line at a generic column j

Several sources of uncertainty affect LLT sensors. They can be classified as:

- **Geometrical:** Any fluctuation of the geometrical quantities in Eq. 10 is a source of uncertainty; the design of LLT sensors therefore aims to keep sensor geometry as stable as possible; deformations due to vibrations, external forces or temperature should be minimized.
- **Optical:** Non-linearities present in camera lenses, laser diodes and laser lenses cause aberrations and distortions which need to be compensated for.
- **Laser-surface interaction:** Laser line image contrast and intensity depend on light scattering at the target surface. Diffuse scattering produces the best images, while mirror-like surfaces reduce laser image intensity, can create artefacts, and make the measurement highly uncertain or impossible; similar problems apply on transparent or highly absorbing surfaces.

2.2 Methods for calibration of laser line triangulation systems

In the applications of the openZDM project, two NDIs will measure straightness on nominally rectilinear steel bars, while one will measure gap and flush on automotive car bodies. In all these cases, we have a target surface which is close to a straight line, being the steel bars nominally straight and the car body parts nominally almost aligned to each other. Instead, the fourth LTT system takes geometric measurements on the finished product, whose geometry is 3-dimensional.

Calibrating an LLT can be done following different approaches: we consider direct calibration methods for LLT as the appropriate ones for our NDIs.

Direct calibration methods are implemented following the procedure outlined in Paragraph 1.5; however, as noted above, an LLT sensor is a 2D sensor, therefore the method has to be implemented taking this into account. Figure 14-c shows that the input to the LLT sensor is a 2D information, the coordinates of the points along the laser line (x, z) , and the corresponding output is the coordinates (i, j) of the image of those points formed on the image sensor. Therefore, the reference input should be an array of known points (x_k, z_k) , with $k=1, \dots, N$.

In general, this array of known input points can be realized by artefacts, having an accurate geometry and allowing a clear and accurate definition of some specific points, mounted on highly accurate traversing stages, so as to position the artefact at known positions in the (x, z) space.

The calibration of the LLT sensor will therefore produce two calibration functions [7],[8], which are 2D polynomials, as those represented in Figure 16. The analysis of the residuals of the calibration data will provide the evaluation of calibration uncertainty.

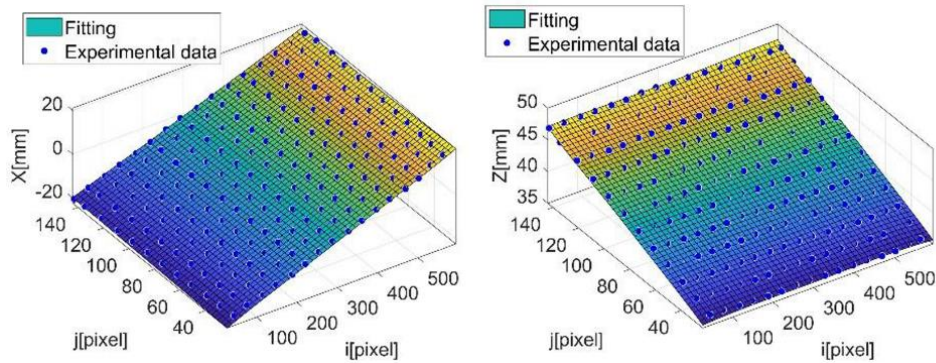


Figure 16: Typical calibration plots for LLT sensors [[8]]

In order to properly implement this calibration method, the calibration target (the artefact) and the traversing stage have to be properly designed.

Different calibration targets can be used for the calibration of the laser line triangulation system. In Figure 17 some examples of calibration targets present in literature are reported.

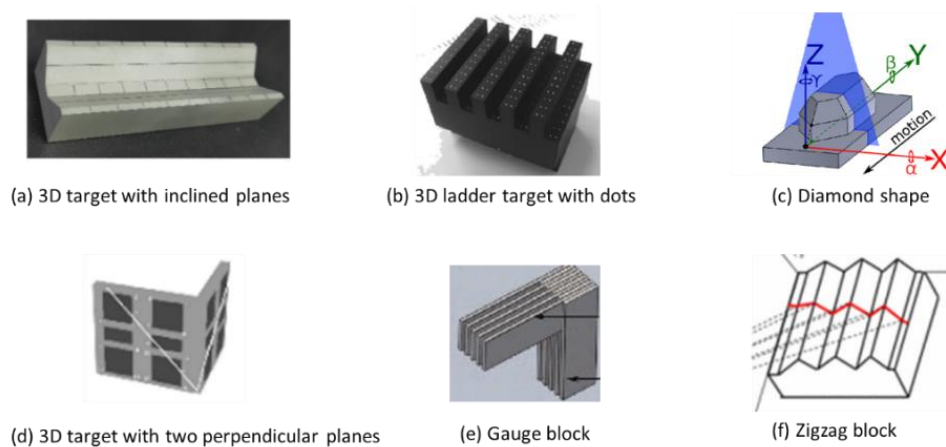


Figure 17: Examples of calibration targets used for LLT sensors (References: figure (a) [9], figure (b) [10], figure (c) [11], figures (d), (e), (f) [12])

In the openZDM project, the design of the calibration bench is different for the different NDIs as described in the following subsections.

2.2.1 Calibration method for laser line triangulation NDI systems for bar straightness

The two NDI systems for bar straightness measurements are laser line triangulation systems that will measure the shape of raw product at different stages of the production process: The first will be installed at low temperature, while the second one will be installed at high temperature. Both these laser line triangulation systems will be used to measure the straightness of the bars and identify potential deviations from the given tolerances. The process of calibration, which allows to finding of a conversion factor pixel/mm, is therefore of primary importance as it will determine the mm unit measured, upon which the conformity assessment is taken to confirm or deny if the product respects the tolerances.

The target used has a trapezoidal shape of the dimension reported in Figure 20 and it is positioned on two linear stages that will allow a 1 mm step in the x and z directions. The LLT sensor is placed on a support in front of the target as represented in Figure 21.

For each step, an image is acquired by the sensor and, for the complete calibration procedure, a total of 154 images are acquired and analysed.

A calibration SW has been developed and as output, the calibration parameters to be stored in the LLT sensor are provided.

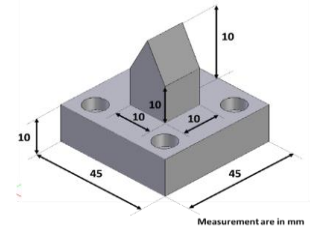


Figure 20: NDI#8 target geometry

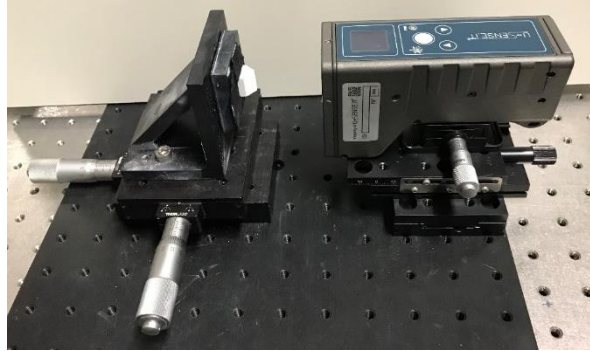


Figure 21: NDI#8 calibration bench.

2.2.3 Calibration method for 3D geometry measurement NDI system with laser line triangulation

The NDI is a laser triangulation system for the 3D dimension measurement of finished products. The system makes use of a robot or a linear positioning guide to move the laser triangulation sensor or the product in order to acquire sequences of laser profiles projected by the laser onto it. For this reason, the NDI can be recalled as a robotised laser triangulation system. Its architecture is sketched in Figure 22. From the laser profiles post-processing, a point cloud of the 3D geometry of the arm can be reconstructed. Since the laser triangulation sensor is a commercial measurement system, laboratory calibration is not required. Each profile in output from the sensor is therefore given in the physical unit, e.g., millimetres both in Y and Z direction (see Figure 22). The distance between the profiles in the X direction depends on the robot's motion and on its position if it can be measured each time a profile is acquired. If one can rely on the accuracy, reliability, and repeatability of the robot in performing prescribed trajectories, calibration of the X coordinate is not required as well.

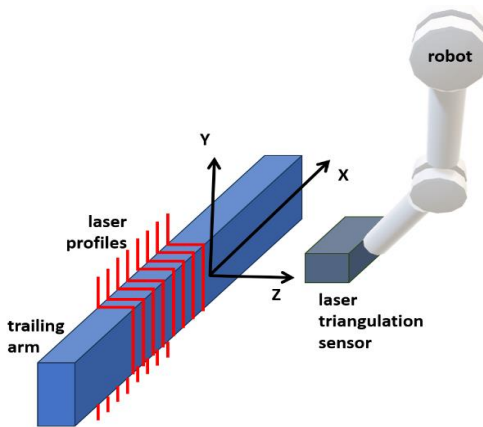


Figure 22: NDI for 3D geometry measurement architecture

3 Uncertainty and calibration methodology for vision-based techniques (VIS and IR) for in-line defect detection

The openZDM project is also focussed on the development and application of NDIs making use of vision systems; some vision systems operate in the visible range, some in the infra-red range. In particular, the under-development NDIs embody vision systems are seven, each designed for a specific application:

- vision in the visible range (3 NDIs):
 - Vision NDI system for surface defect detection;
 - Camera NDI system for gob quality assessment;
 - 2D Camera NDI system for welding process monitoring.
- vision in the infra-red range (4 NDIs):

- Two thermographic measurement NDI systems for temperature distribution measurements of incandescent bars;
- Thermal camera NDI system for glass bottle thickness measurement;
- IR Thermal camera NDI system for detection of welding process defects.

In the use cases of the openZDM project, vision in the visible range (NDI#6, NDI#9b and NDI#11) is applied to detect geometrical features, i.e., surface defects of steel bars such as scratches and bumps, the 2D shape of high-temperature gobs and aesthetical defects of welded joints, such as holes and bad couplings. Therefore, these vision systems in the visible range should be calibrated in the object space domain, in order to provide accurate geometric information; this is done through a classical camera calibration procedure, a geometric calibration that can be implemented at different levels of accuracy, depending on the requirements of each case.

On the other side, vision systems in the infrared range are used for different purposes, which pose different and specific requirements for calibration:

- The two thermographic measurement NDI systems for temperature distribution measurements aim to measure surface temperature distributions on hot steel bars. This requires calibration in the intensity domain, being image intensity related to infrared emission, which in turn depends on object temperature and surface emissivity. At the same time, geometric calibration in the object space domain is less relevant, unless severe distortions are observed, because these NDIs are not required to perform geometric measurements.
- The thermal camera NDI system for glass bottle thickness measurement aims to indirectly measure glass bottle thickness through the intensity of infrared emissions. This requires a calibration of image intensity vs. bottle thickness. In addition, this NDI will make use of a deep learning-based model, trained to learn the relationship between the infrared emission (pixel intensity value) together with other variables of the manufacturing process; therefore, calibration, in this case, refers to training the neural network with annotated (ground truth) data of the thickness of some selected bottles. The requirement for the measurement system is to keep a stable sensitivity to infrared radiation and be robust against disturbances such as reflected radiation from hot sources nearby.
- The IR thermal camera NDI system for the detection of welding process defects aims to perform an inspection over an electrical resistance; local overheating represents a defect. Also, in this case, the scope is to detect the presence of a defect, not its geometry, and a neural classifier is used. Therefore, also in this case, calibration refers to training the neural network and uncertainty refers to false positives or false negatives. The requirement for the measurement system is to keep a stable sensitivity to infrared radiation and be protected against disturbances such as reflected radiation from hot sources nearby.

3.1 Uncertainty in vision systems

Two fundamental types of uncertainty affect vision systems: a) image geometry distortion and b) image intensity uncertainty.

Uncertainty due to image geometry distortion arises from factors such as lens aberrations, camera lens misalignment, three-dimensional objects and perspective projection, which altogether cause image distortion. These issues can alter the spatial relationships between objects in an image, making it challenging to accurately measure distances and angles.

Different types of distortion are possible, such as:

- *Perspective distortion*: parallel lines appear to meet due to perspective.
- *Radial distortion*: straight lines seem to curve over the image.
- *Tangential distortion*: occurs because of an angular misalignment between the image plane and lens and manifests as a leaning or slanting effect in the image.
- *Pin cushion distortion* (Figure 23): objects located in the centre of the frame appear normal, but those located along the edges of the image appear to be squashed toward the centre.
- *Barrel distortion* (Figure 23): contrary to pincushion distortion, objects in the centre of the image appear normal, but those located along the edges of the image appear to expand outward.

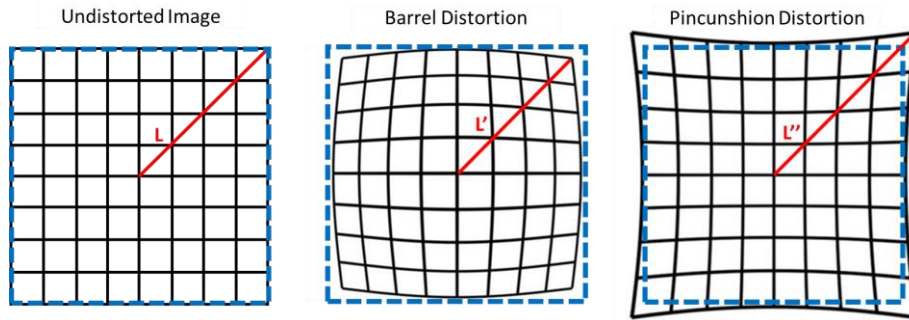


Figure 23: Example of typical image distortions

Camera calibration allows compensation of these effects. Camera calibration is done according to one of the variants of the method presented by Zhang, which identifies intrinsic and extrinsic parameters of the camera by analysis of the sequence of images of a reference target, usually a checkerboard [16].

On the other hand, **image intensity uncertainty** can also pose significant challenges. It refers to the lack of precision or variability in measurements of pixel intensity or colour values within an image. This uncertainty can result from several sources, including errors in image sensors, noise in data acquisition, imperfections in illumination, reflections, and so on. For instance, in infrared imaging, a thermal camera needs to be calibrated to correlate what the camera sees with known temperatures. For example, the user of a thermal vision system must pay special attention to determining the emissivity value of the surface under analysis if quantitative measurements are required. In addition, the problem of uncertainty in image intensity can be further exacerbated by environmental factors such as reflections, absorption along the optical path, occlusions, and dynamic changes in the scene.

In particular, the overall temperature uncertainty ΔT performing infrared measurement is the sum of different contributions, see Figure 24:

- Uncertainty ΔT_{ϵ} related to the emissivity of the object.
- Uncertainty ΔT_A caused by radiation **absorption** along the optical path (the purple opaque obstacle in the path between the object under test and sensor blocks part of the radiation by absorbing it).
- Uncertainty ΔT_{RT} caused by **reflections** (the radiation of a spurious radiation source is reflected by the window placed in between the object and the sensor and collected by the sensor) and radiation **transmission** (a portion of the radiation from the object under test is reflected by the same window and sent away from the sensor;).
- Uncertainty ΔT_S of the **sensor**.

Emissivity uncertainty is the main cause of uncertainty in T measurements by infrared instruments.

Emissivity characterizes how efficiently an object emits thermal radiation. It can vary depending on the material, surface properties (e.g. roughness), angle of view, temperature of the object, wavelength, and so on.

On the other side, to better understand what issues related to absorption, transmission, and reflection consider the effects depicted in Figure 24. If the emitted infrared radiation encounters reflective surfaces or materials along the optical path, some of it may be reflected and not reach the sensor. This reflected radiation introduces uncertainty if it is not properly accounted for.

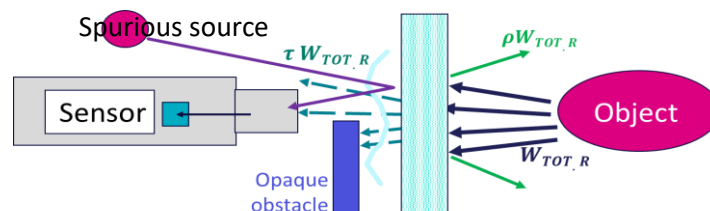


Figure 24: Problems related to absorption, transmission, and reflection

Similarly, the infrared radiation could pass through materials before reaching the sensor. Typical interposed mediums are atmospheric air, windows for optical access, any gases, etc. The resulting effect is that less energy reaches the sensor from the body than is emitted by the object, due to the absorbance (α) of the medium (Figure 25).

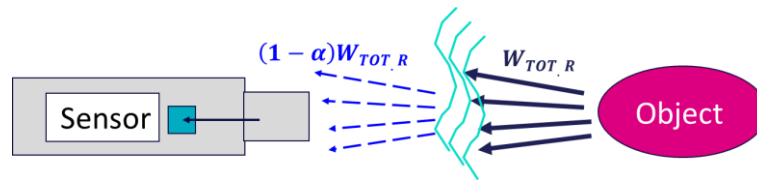


Figure 25: Uncertainty due to radiation absorbed in the path from the object to the sensor

In addition, more energy could come to the sensor from the environment, as Figure 26 shows. There may be other sources in the environment whose infrared radiation should not reach the sensor, such as the presence of a furnace. In such cases, the source should be shielded. Alternatively, the sensor, or the interposed reflective window, could be rotated to make the optical path of the interfering radiation change.

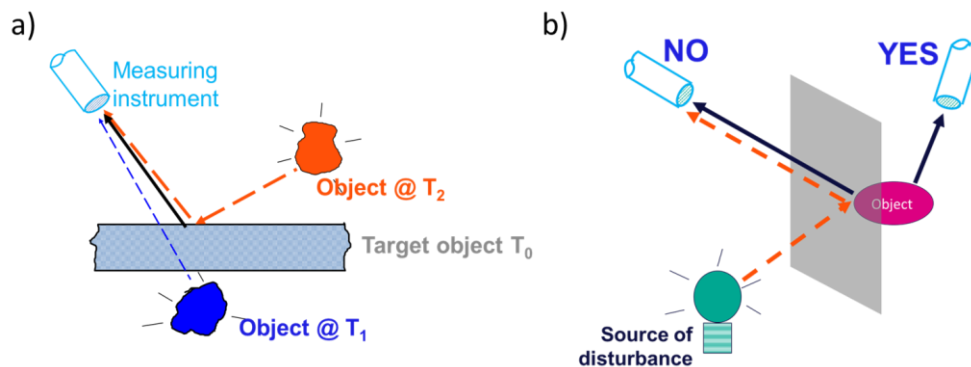


Figure 26: a) Example of interfering radiation sources: reflected (orange path) and transmitted radiation (blue path). b) Solutions against environmental interference

The accuracy of the sensor itself is crucial. This includes factors such as calibration drift over time and sensor noise. Proper calibration and maintenance are necessary to minimize uncertainty due to the sensor.

3.2 General methods for vision systems calibration

3.2.1 Spatial calibration of vision systems

Calibration of vision systems is primarily concerned with spatial relationships to the image, correcting distortions caused by camera optics and ensuring accurate measurement of distances and angles. It allows pixels to be expressed in metric units [mm]: a single scaling factor for the entire scene [mm/pixel] is sufficient if there are no causes of image distortion, while a matrix transformation is necessary to describe situations where image distortion is relevant. Calibration is particularly important for tasks such as 3D reconstruction, object tracking, and accurate object sizing.

Calibration should lead to find the transformation matrix M such that:

$$\mathbf{P}: [X, Y, Z] \xrightarrow{M} \mathbf{p}: [x, y] \quad \text{Eq. 11}$$

Where $[X, Y, Z]$ are world coordinates and $[x, y]$ are pixel coordinates in the acquired image.

To find the transformation matrix (Eq. 11), two groups of parameters are needed:

- Extrinsic parameters, related to the installation of the camera in space (position and orientation)
- Intrinsic parameters, related to the camera's characteristic features, such as effective focal length, sensor position, and pixel size.

To perform this calibration, it is necessary to know the location of many points in world coordinates and then to be able to relate these points to their counterpart in the image. To facilitate this process, objects with easy-to-locate and extract points are generally used, e.g., checkerboards. An example of a checkerboard is shown in Figure

27. If the camera is an infrared camera, it is necessary to make the checkerboard in such a way that in the infrared the known points are easily detectable. The checkerboard for systems in the infrared is shown in the figure, and aluminium squares and squares with black absorbing tape are alternated, such that they emit differently in the infrared.



Figure 27: a) Checkerboard for visible systems, b) checkerboard for infrared systems, c) infrared image of the checkerboard for infrared systems

Using an appropriate calibration algorithm, it will be possible to calculate the camera matrix, using extrinsic and intrinsic parameters: extrinsic parameters transform world points into camera coordinates, and intrinsic parameters project camera coordinates into the image, as shown in Figure 28.

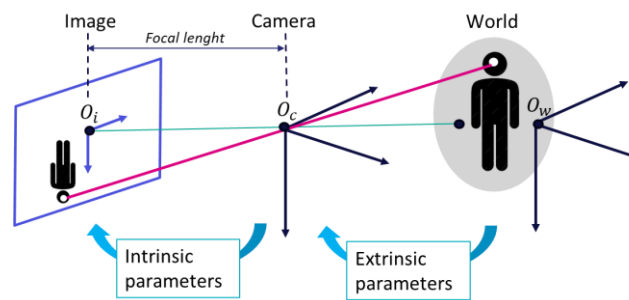


Figure 28: Role of extrinsic and intrinsic parameters image formation

3.2.2 Intensity calibration of infra-red vision systems

For IR vision systems, in addition to geometric calibration (not always necessary), the challenge is to quantify the ability of a surface to emit in the infrared, that is, to determine the correct emissivity value. The intensity of radiation emitted by an object is a function of temperature T and emissivity ε : $I(x, y) = f [T(x, y), \varepsilon(x, y)]$

To determine the emissivity of a material, it is essential to use a reference either in terms of temperature or emissivity.

Using a temperature reference means using a contact sensor (such as a thermocouple) to determine the correct temperature value of the object. Then the emissivity value is changed until the value read on the thermal camera matches the value on the reference thermocouple. Be careful to place the thermocouple at a point immediately next to the one measured with the thermal camera, where the actual temperature is the same.

On the other hand, using an emissivity reference means using a paint of known emissivity or an adherent material of known emissivity on the measurement object. The object and the reference, being in contact, are at the same temperature, but because they have different values of emissivity, they will appear at different temperatures in the thermal image. Again, the emissivity of the unpainted object will have to be changed until the read temperature is the same as that of the reference.

It is very important to determine emissivity under real measurement conditions since, as mentioned before, it depends on many factors, most of which are related to the measurement environment.

The main component of both thermographic measurement NDI systems for temperature distribution measurements is a thermal camera with a near-infrared wavelength range between $0.85 - 1.1 \mu m$. the camera frames the incandescent bar after the heating stage of trailer suspension arms in the VDLWEW production process.

The calibration of the emissivity of the bar surface material has been performed in the UNIVPM laboratory as reported in Figure 29.

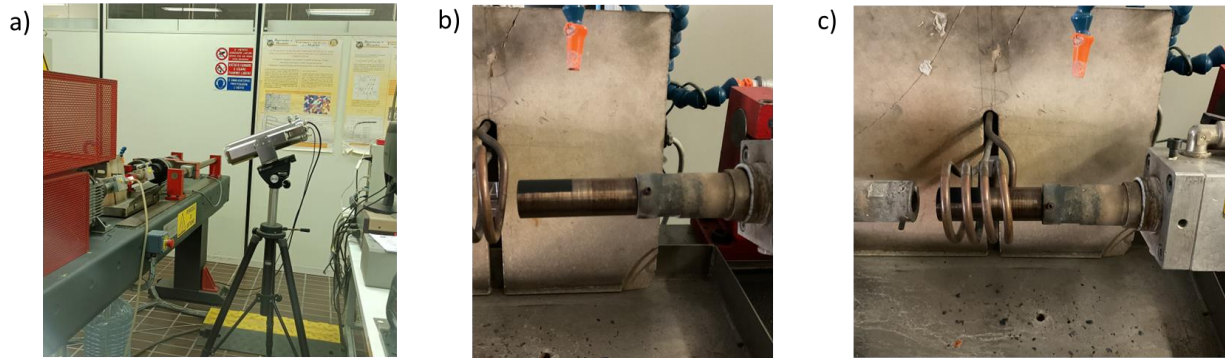


Figure 29: a) UNIVPM emissivity calibration setup. b) Partially painted sample. c) Setup for heating the sample.

Particularly, an emissivity reference has been used: the steel sample has been partially painted in Figure 29 (b) with a high-temperature resistant paint with known emissivity at different temperature values. Then, the sample has been heated to 1100°C Figure 29 (c). The temperature values of the painted and unpainted surfaces were compared. The emissivity of the sample was then determined by modifying the emissivity of the unpainted bar in the image until the same temperature was registered over the unpainted and painted portions.

3.2.3 Intensity calibration for NDIs exploiting neural networks

The thermal camera NDI system for glass bottle thickness measurement and the IR Thermal camera NDI system for detection of welding process defects exploit a deep-learning model to provide the output information; in this sense, the input-output relationship that typically characterizes a measurement instrument includes a step involving an Artificial Intelligence (AI). Therefore, calibration in this context is something different and the methodology that will be implemented is as follows.

In particular, for the first NDI which uses a deep learning-based model, calibration will consist of training the system to learn the relationship between the infrared image intensity and the thickness of the bottle at the end of the process; the neural model considers also other variables of the manufacturing process. In this perspective, the reference input used for calibration is constituted by some selected bottles, having known thickness, in practice by annotated data (ground truth).

Similarly, in the second NDI, the objective is to detect the presence of a defect in the weld. In order to perform such a diagnosis, a neural classifier is used. Again, calibration in this case refers to training the neural network to recognize the presence of defects; this is not the typical calibration process as meant in metrology. Also, the concept of uncertainty is different from metrology. In this diagnostic process, uncertainty refers to false diagnoses, which can be either false positives or false negatives.

For both NDIs, the requirement for the measurement system (the thermal camera) is to keep a stable sensitivity to infrared radiation and be protected against disturbances such as reflected radiation from hot sources nearby.

4 Uncertainty and calibration methodology for X-ray instrumentation for residual stress developed

OpenZDM is also focused on the development and application of NDIs making use of x-rays to measure residual stress of steel bars. In particular, residual stress is measured in two different sections of the production line, thus resulting in 2 NDIs:

- X-ray residual stress detection of raw bars;
- X-ray residual stress detection of processed bars.

The manufacturing and transformation processes of metallic materials generate variations in the microstructure and consequently variations in their physical properties. Thermal processes (hot rolling, welding, forged, and others), and mechanical processes (bending, machining, and others) generate plastic deformation and residual stresses in the metallic materials. Elastic deformations in metals that have crystalline structures can be

determined by measuring their lattice parameters using X-ray diffraction, which is based on the measurement of the distance of the atomic planes (d), whose value in the undeformed state is known. Procedures based on this technique have the advantage of being non-destructive. Figure 30 shows the reflection of an incident beam and Eq. 12 shows the Bragg Law condition.

Considering the laws of diffraction, angle θ , is the same for the incident beam as for the reflected beam, only those atomic planes perpendicular to the bisector S , between the incident beam and the reflected, participate in the diffraction. Thus, S is considered as the direction of the diffraction measure.

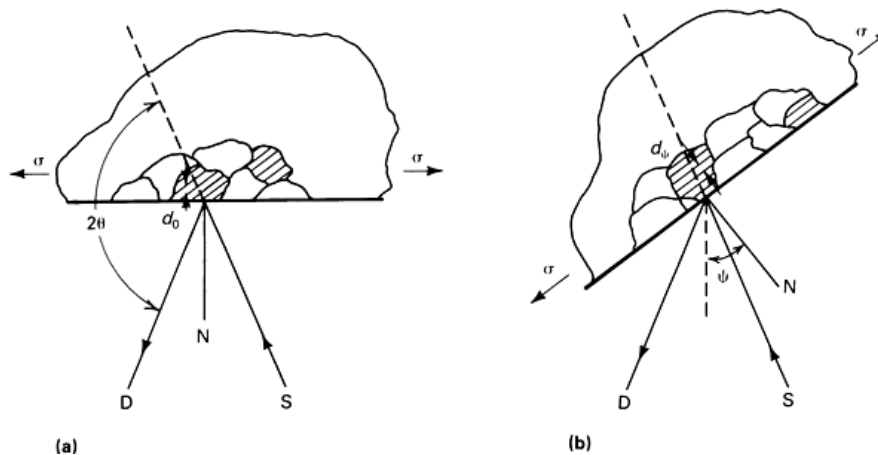


Figure 30: Direction of measurement in x-ray diffraction where n : = reflection order, λ : = wavelength, $d \sin \psi$: =distance between two planes oriented according to (hkl) and θ : = angle of diffraction [17]

$$2d \sin \theta = n \cdot \lambda \quad \text{Eq. 12}$$

Where: d is the interplanar space, θ is the angle incident beam and λ is the X-ray wavelength

For reasons of focusing of the reflected beam in the conventional detector diffraction equipment maintains the direction of measurement S , perpendicular to the surface of the sample (Figure 30 a), simultaneously varying during the sweep the angle α of the incident beam with the sample and the angle β of the direction of the detector with the sample. In this case α and β are both equal to θ and the planes are parallel to the surface. To detect families of planes, that form an angle $\psi \neq 0$ with the surface, it is necessary to move the measurement direction by the same angle with respect to the normal surface (Figure 30 b), $\alpha \neq \beta$ and both different from θ . The angle between the detector direction and the incident beam extension, however, it is still 2θ and consequently the corresponding value of d can be determined in the new S .

The iXRD system in Figure 31 uses two detectors, that geometry allows higher tilt angle and reduces defocusing problems. This system, used for the purposes of openZDM, uses a modular mapping in laboratory configuration. With this equipment, the triaxial method is used, where measurements are made in different Φ directions (Φ angle: is the angle rotation perpendicular to the sample surface (0-360°) and all possible β angles.



Figure 31: iXRD system with modular mapping

4.6.1 Triaxial method:

This method uses various Φ angles, (usually 0°, 45°, and 90°) at each of these angles, 13 β angles are measured under the next conditions:

- X-ray tube: Cr K alfa
- Power: 20 Kv y 4 mA;
- Colimator: AP-1,0mm;
- β angles:13;
- Φ angles:3;

- Number of exposures: 20;
- Exposure time: 2 s;
- Peak location method: Gaussian 75%.*

* The diffraction peak can also be represented by a mathematical function, the most common being Gaussian. Peak height is cut at 75-80%.

The stress tensor, principal stress, direction of the principal stress, shear stress, and equivalent stress are calculated with this method.

- **Stress tensor:** it is a mathematical representation in matrix form (Eq. 13) of the stress state to which a point on a piece is subjected. The stresses expressed by the stress tensor are associated with an orthogonal reference system defined at said point.

$$\sigma_{XYZ} = \begin{bmatrix} \sigma_{xx} & \tau_{xy} & \tau_{xz} \\ \tau_{xy} & \sigma_{yy} & \tau_{yz} \\ \tau_{xz} & \tau_{yz} & \sigma_{zz} \end{bmatrix} \quad \text{Eq. 13}$$

The stress tensor is symmetrical, and each row or column shows the three stresses (1 normal and 2 shear stresses) associated with the plane perpendicular to each axis of the coordinate system.

- **Principal stress:** Principal stresses at a point in a loaded body are the normal stresses in the principal directions at that point. The maximum of these principal stresses (σ_1) is the maximum normal stress of all stresses occurring when the orientation of the plane at that point is changed. Similarly, the minimum is the minimum normal stress (σ_3) of all the stresses that can occur when changing the plane orientation at that point. The calculation of principal stresses and directions is equivalent to a diagonalization of the stress tensor at the point (Figure 32).

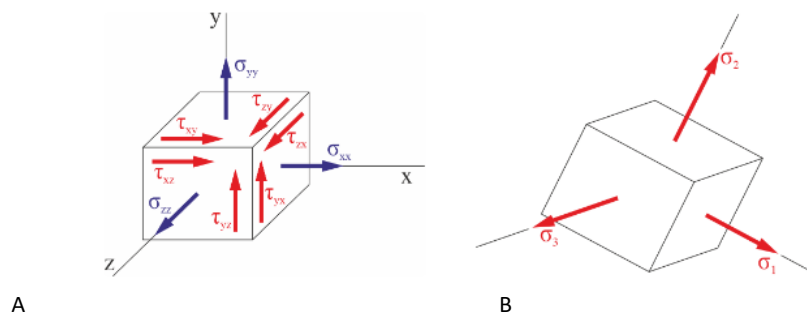


Figure 32: Distribution forces, and the stresses they cause, on the forces of a homogeneously loaded unit cube at static equilibrium. Schematic representation of tensional state at one point (a) and principal stress and directions at the same point [18]

- Direction of the principal stress: this value indicates the direction of the principal stress measured, with respect to the direction taken as Φ zero.
- Shear stress: normal stress is calculated from the slope of d vs $\sin^2\psi$. The shear stress is evaluated from d vs $\sin^2\psi$ plots. The shear stress can be seen when the material is machined, for example. This is related to the heterogeneity of the microstructure of the material (non-uniform strain). For instance, the shear component is higher in high-carbon steel than low-carbon steel (Figure 33).
- Equivalent stress: is used as it combines the 9 values in the matrix. It is considered more accurate than maximum stress, as it takes into account the interaction between the three stress components.

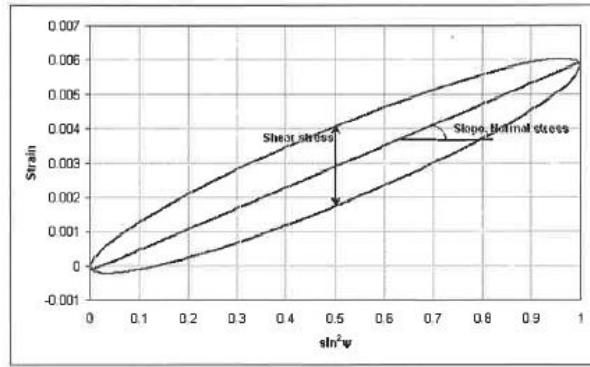


Figure 33: " 2θ vs. $\sin^2\Psi$ curve, calculation of normal stress" and shear stress

4.1 Uncertainty of X-ray Residual Stress measurement

The uncertainty in residual stress measurements can be divided into two components: that related to the statistical process and that caused by the measurement process (alignment of the diffractometer and specimen displacement).

4.1.1 Uncertainty related to statistical processing

The diffraction peak position must be established by a curve fitting method which introduces some uncertainty in the results. The strain data obtained must be transformed into stresses using elastic constants. There may also be problems of non-linearity due to texture, coarse grain size, stress gradients with depth, and micro-stresses due to plastic deformation or grain interactions. Many of these are non-quantifiable although theoretical analyses and modelling are being developed to solve these problems. Some of the experimental and analytical methods dealing with these non-linearities introduce their own error contributions. In our case, Proto's software estimates an error related to all these parameters in each individual measurement taking into account this lack of linearity and the associated curve fitting errors.

4.1.2 Effect of system misalignment on stress results:

Misalignment of equipment can have a number of negative effects:

Misalignment produces translation and beam shift, that result in characteristic shapes of the curves as shown in Figure 34 and Figure 35.

Figure 34 Figure 35

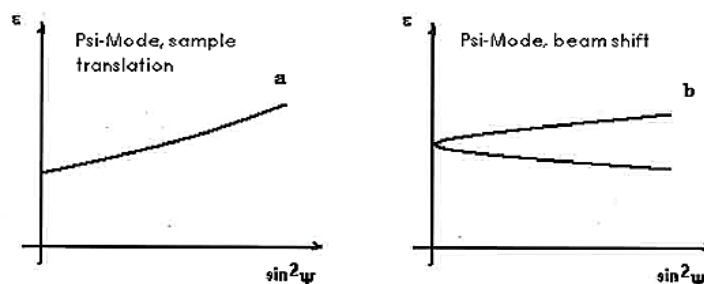


Figure 34: Effect of beam shift and sample translation on the shape of $\sin^2\Psi$ curve, and Ψ -mode. Presence of (a): normal stress only and (b): shear stress only [18]

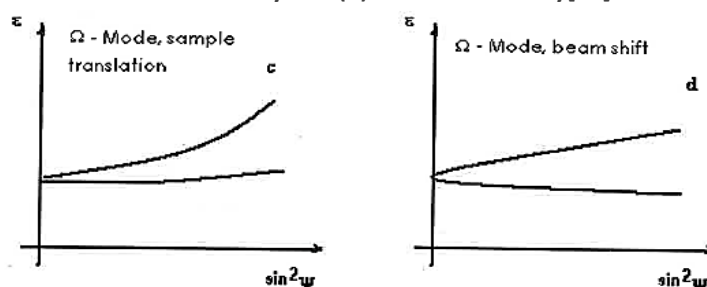


Figure 35: Effect of beam shift and sample translation on the shape of $\sin^2\Psi$ curve, and Ω -mode. Presence of (c): normal and shears stress and (d): shear and shears stress [19]

4.1.3 Effect of specimen displacement:

When a sample is displaced by a certain amount from the centre of a goniometer, fictitious stress usually adds to real stress. This is caused by the fictitious peak shift due to misalignment. This is the case when the sample is translated by a distance d_0 from the centre of rotation close to the incident beam or away from the incident beam.

4.2 Calibration of X-ray residual stress measurement

The X-ray diffraction residual stress measurement system requires proper alignment of all moving parts to ensure correct measurement. The use of "standards" is used to verify the correct alignment of the equipment.

In general, we say that Rx diffraction as an absolute method does not need other methods to calibrate, as it is a reference method for other techniques. In summary, we can say that this technique does not require calibration.

The procedure for the alignment of the Beta movement of the equipment is performed manually. The alignment of the Beta movement of the unit is performed as follows:

- Mount the microscope on the table or on a rigid surface. Secure its position using mounting screws or other means to keep it at an absolute fixed position;
- Focus the microscope on the end of the pointer. The distance is approximately 2.5 cm away;
- Turn the flashlight to illuminate the white screen behind the pointer;
- Using the XRDWIN software move the beta motor to -35° . As the motor is moving view the movement of the pointer in the eyepiece. Move the motor to $+35^\circ$ and watch the movement of the pointer in the eyepiece. If the system is aligned the pointer will not move but rotate about the centre of the eyepiece. The alignment is good if the pointer stays within 2 circles of the centre. If the system is out of alignment, then the pointer will not stay centred in the eyepiece but move in an arc about the centre.

Figure 36, Figure 37 and Figure 38 show the different positions for the pointer with beta angles equal to: a) -35° , b) 0° , c) $+35^\circ$. Similarly, the path of the pointer is shown in e).

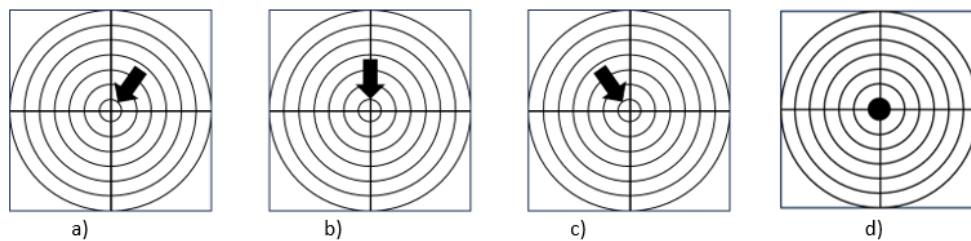


Figure 36: Good alignment [20]

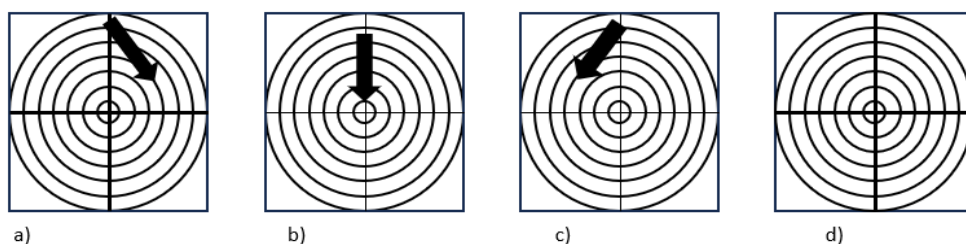


Figure 37: The system is out of alignment and needs to be moved up [20]

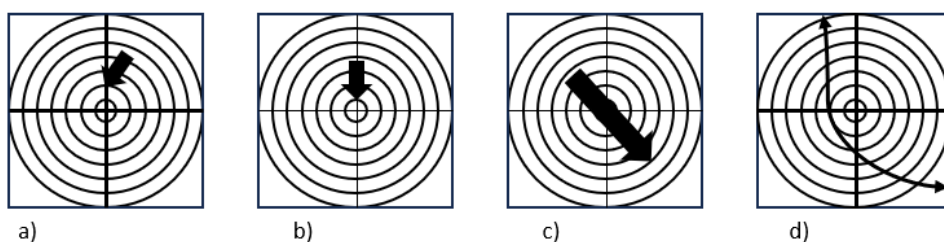


Figure 38: The system is out of alignment and needs to be moved down and left [20]

Once the equipment is aligned, one can proceed to the alignment verification. Verification is performed by inspection of a specimen of iron powder, which in the case of the equipment used in NDI0 is provided by the manufacturer. This specimen is a stress-free sample on which 5 measurements must be performed. If the equipment is well aligned, the systematic error of the 5 measurements will be ± 14 MPa. Similarly, it has been proven that if the equipment is well aligned, the standard deviation of the 5 measurements should not exceed ± 7 MPa.

5 Pathway for implementation and concluding remarks

This document has provided an overview of the concepts of measurement uncertainty and calibration, addressing the measurement technologies used for the various NDIs under development. Then, for each type of measurement technique used in the project, the deliverable has described the methodologies for calibration that are currently being implemented.

In particular, the action plan for the complete development of the NDI and for its calibration is as follows.

- For the laser line triangulation NDI systems for bar straightness, the direct calibration method outlined is being implemented, using a saw-tooth reference target. The calibration software has been developed and tested on laboratory prototypes of the NDIs. A re-engineered version of the NDIs is almost completed and assembled which will be then calibrated in the same manner.
- For the IIoT portable laser line triangulation NDI system for gap and flush measurement, the direct calibration method outlined is being implemented, using a small trapezoidal target. The initial prototype has already been calibrated, and the new engineered version is available and will undergo the same calibration process.
- For the A 3D geometry measurement NDI system with laser line triangulation on a robot, the two configurations developed and tested have been compared; robot trajectory affects the uncertainty of measurements and needs to be corrected, however, corrections did not allow to achieve the desired accuracy in 3-D measurements over the finished suspension arm. Therefore, a new version is under design, which uses a linear stage for scanning the laser sensors along the trailing arm; this development will be implemented depending on available resources and it is considered highly challenging and, therefore risky.
- For two thermographic measurement NDI systems for temperature distribution measurements of incandescent bars, which are thermal cameras operating in the Near Infra-Red region to measure the temperature of incandescent steel bars, it has already been performed calibration for emissivity. Now one NDI is already installed in-line, taking measurements continuously; the data collected are being used to assess if the system performance is stable, if dirt affects calibration and if re-calibration is necessary or if drift compensation can be implemented. The other NDI will be later installed and will follow the same process in terms of calibration and uncertainty estimate.
- For the NDI using X-ray for residual stress measurement, which is a visible range inspection system of surface defects, the camera acquisition parameters have been optimized in the design and setup phase, selecting optics, sensor characteristics and camera position that meet the requirements for field of view and defect resolution. Based on laboratory testing, we expect to resolve up to 0.5mm wide defects. When deployed at the factory, the camera setup will be fine-tuned to optimise contrast highlighting defects. Full projective camera calibration will not be needed, since the system will detect 2D surface anomalies without performing geometric measurements.
- For the thermal camera NDI system for glass bottle thickness measurement, which is an expert system to predict the thickness of the bottle, the availability of historical data from thermal images and final quality measurement and thickness indicators is essential for training and calibration of the expert system planned in the NDI. After several months, it is now possible to collect data with 1:1 identification. It is expected to include different bottle models in the analysis. However, there are more variables that influence the quality of the bottle and for this reason, a parallel analysis is being carried out that includes the gob data and other signals from the production line. The findings of this analysis will be part of the camera NDI system for gob quality assessment.
- For the camera NDI system for gob quality assessment, which is an expert system to evaluate the overall quality of the bottle from the influence of the gob and other line parameters, a preliminary exploration has been achieved. The NDI takes images of gobs, extracts gob features by image processing techniques and tries to find correlations between these characteristics and the final thickness values of the bottles. Unfortunately, there is

no 1:1 dataset traceability, so approximate averages in different time periods are considered. Just preliminary correlations have been found and findings should be ensured with larger data sets. For this NDI, not all the data is coming from the same production plant, and available information is then coming from different sources, not synchronized between them.

- The 2D camera NDI system for welding process monitoring and the IR thermal camera NDI system for detection of welding process defects are based on deep-learning models to classify welding defects; therefore in this case a typical image calibration is not required because they do not perform geometry measurement. The next step will be to perform the training of the neural model in order to build the diagnostic model.
- For both X-ray NDIs for residual stress detection it is currently performed a verification of calibration by reference standards each time measurements are taken, as required for this type of laboratory equipment.

References

- [1] Joint Committee for Guides in Metrology (JCGM) website <https://www.iso.org/sites/JCGM/JCGM-introduction.htm>
- [2] Bureau internationale de Poids et Mesures (BIPM) website <https://www.bipm.org/fr/home>
- [3] ISO-GUM JCGM 100 series – Guides to the expression of uncertainty in measurement (GUM series), available online at <https://www.iso.org/sites/JCGM/GUM-introduction.htm>
- [4] JCGM 100:2008, Evaluation of measurement data — Guide to the expression of uncertainty in measurement (GUM), available online at https://www.bipm.org/documents/20126/2071204/JCGM_100_2008_E.pdf
- [5] JCGM 200 – International vocabulary of metrology Basic and general concepts and associated terms (VIM), available online at <https://www.iso.org/standard/45324.html>
- [6] ISO-10012:2003 « *Measurement management systems — Requirements for measurement processes and measuring equipment* »
- [7] ISO 14253-1-2017 « *Geometrical product specifications (GPS) -- Inspection by measurement of workpieces and measuring equipment -- Part 1: Decision rules for verifying conformity or nonconformity with specifications* »
- [8] E.Minnetti, P.Chiariotti, N.Paone, G.Garcia, H.Vicente, L.Violini, P.Castellini, “A Smartphone Integrated Hand-Held Gap and Flush Measurement System for in Line Quality Control of Car Body Assembly”, *Sensors*, 20, 3300; 2020, doi:10.3390/s20113300
- [9] Wu, Xiaojun & Tang, Na & Liu, Bo & Long, Zhili. (2020). A novel highly precise laser 3D profile scanning method with flexible calibration. *Optics and Lasers in Engineering*. 132. 105938. 10.1016/j.optlaseng.2019.105938.
- [10] Xu, Xiaobin & Fei, Zhongwen & Yang, Jian & Tan, Zhiying & Luo, Minzhou. (2020). Line structured light calibration method and centerline extraction: A review. *Results in Physics*. 19. 103637. 10.1016/j.rinp.2020.103637.
- [11] <https://www.automationtechnology.de/cms/en/support-packages/>
- [12] X. Zhang and J. Zhang, "Summary on calibration method of line-structured light sensor," 2017 IEEE International Conference on Robotics and Biomimetics (ROBIO), Macau, Macao, 2017, pp. 1142-1147, doi: 10.1109/ROBIO.2017.8324571.
- [13] F. J. Duan , F. M. Liu, Sh. H. Ye. "A New Accurate Method for the Calibration of Line Structured Light Sensor", *Chinese Journal of Instrument Scientific*, vol.21, no.1, pp.108-110, 2000
- [14] P.Castellini, A.Bruni, N.Paone, “Design of an optical scanner for real-time on-line measurement of wood-panel profiles”, 18th Int. Congress on Photonics in Europe, Optical Metrology, Munich, Germany, 18-21 june 2007, *Optical Measurement Systems for Industrial Inspection V*, edited by W.Osten, C.Gorecki, E.L.Novak, Proc. of SPIE Vol. 6616, 66164E, (2007) · 0277-786X/07/\$18 · doi: 10.1117/12.725042
- [15] ISO/IEC 17025 - General requirements for the competence of testing and calibration laboratories available online at <https://www.iso.org/standard/66912.html>

- [16] Zhengyou Zhang, “A Flexible New Technique for Camera Calibration”, Technical Report MSR-TR-98-71, Microsoft Corporation, 1998, available online at <https://www.microsoft.com/en-us/research/wp-content/uploads/2016/02/tr98-71.pdf>
- [17] Prévéy, Paul S. “X-ray Diffraction Residual Stress Techniques,” Metals Handbook. 10. Metals Park: American Society for Metals, 1986, 380-392.
- [18] http://www.mecapedia.uji.es/pages/tensiones_principales.html..
- [19] PROTO RESIDUAL STRESS DETERMINATION USING X-RAY DIFFRACTION TECHNIQUE. M. Belassel. Proto manufacturing Limited. 2006.
- [20] PROTO RESIDUAL STRESS ANALYZER. Hardware Manual. Proto manufacturing Limited. 2006.

